DEPOSITION CHAMBER FOR THIN FILM DEPOSITION

By

Kyle R. Flemington

A thesis submitted in partial fulfillment of the requirements for the degree of

Bachelor of Science

Houghton College

June 2015

Signature of Author……………………………………………..……………………..
Department of Physics
June 9, 2003

……………………………………………………………………………………..
Dr. Brandon Hoffman
Associate Professor of Physics
Research Supervisor

……………………………………………………………………………………..
Dr. Mark Yuly
Professor of Physics

DEPOSITION CHAMBER FOR THIN FILM DEPOSITION

By

Kyle R. Flemington

Submitted to the Department of Physics
on June 9, 2015 in partial fulfillment of the
requirement for the degree of
Bachelor of Science

Abstract

The study of thin films has been pertinent in the semiconductor industry for some years now. Research is being done in order to attain a greater understanding of the physical characteristics of thin films. In order to evaporate the metal of interest, a physical vapor deposition process is used. A sample metal is vaporized using an electron beam, the metal then condenses on a substrate with a diameter of 4 inches forming a thin film. This chamber has the capability to make gradient films to study the effect thickness has on texture transformations using physical vapor deposition. It also includes an evaporation rate monitor with a similar design to an ion gauge. In order to ensure deposition onto clean substrates, a Commonwealth Scientific Company Mark I ion mill will be used to clean before deposition.

Thesis Supervisor: Dr. Brandon Hoffman
Title: Associate Professor of Physics

TABLE OF CONTENTS

Chapter 1 Introduction 6
1.1 Thin Films 6
1.2 History of Vacuum Systems 6
1.3 History of Thin Films and PVD 8
1.4 Monitoring Evaporation Rate 12
1.5 Current Understanding of Thin Films 14
1.6 Thin Film Research at Houghton 18
Chapter 2 Aparatus 20
2.1 Introduction 20
2.2 Evaporator 20
2.2.1 Transformer and Rectifier Circuit 20
2.2.2 Designing New Evaporator 24
2.3 Rate Monitor 25
2.4 Pumps 27
2.4.1 Rough 27
2.4.2 Turbo 28
2.4.3 Ion 29
Chapter 3 Analysis 31
3.1 Results 31
3.1.1 First Film 31
3.1.2 Second Film 32
3.1.3 Third Film 32
3.1.4 Fourth Film 33
Chapter 4 Conclusion 34
4.1 Current Status 34
4.2 Future Plans 34
Appendix A Procedures 36
A.1 Evacuation Procedure 36
A.2 Venting Procedure 36

A.3 Bake Procedure **36**
A.4 Deposition Procedure **37**

TABLE OF FIGURES

Figure 1. Gaede's Rotary Mercury Pump. 7
Figure 2. W. Grove's apparatus with which he discovered thin films. 9
Figure 3. Edison's device for making phonographs. 10
Figure 4. Electron beam vaporization via thermionic heating of a crucible. 11
Figure 5. Focused E-Beam Evaporation configuration. 12
Figure 6. A physical sputtering system. 13
Figure 7. A faced-centered cubic crystal. 15
Figure 8. Diagram showing the planes that the (1 0 0) and (1 1 1) Miller indices describe. 15
Figure 9. Miller indices, (1 0 0) and (1 1 1) orientations. 16
Figure 10. The current theory for texture transformation showing a critical thickness. 17
Figure 11. Data taken on texture transformation shows this trend. 18
Figure 12. Houghton College PVD chamber showing locations of aspects of the chamber. 19
Figure 13. Inside of the deposition chamber. 21
Figure 14. The evaporator. 22
Figure 15. Circuit diagram for the entire electronics set-up for the evaporator. 23
Figure 16. The new evaporator. 24
Figure 17. Top view of the top plate that holds the crucible. 25
Figure 18. Diagram of Houghton College's Evaporation Rate Monitor (ERM). 26
Figure 19. A Photo of Houghton College's Evaporation Rate Monitor (ERM). 26
Figure 20. Diagram of Evaporation Rate Monitor (ERM) presented by Geidd and Perkins. 27
Figure 21. The Rotary Vane Pump. 28
Figure 22. Cross-section diagram of the turbomolecular pump. 29
Figure 23. Diagram of an ion pump. 30

Chapter 1

Introduction

1.1 Thin Films

Thin films are defined as materials whose planar dimensions are much larger than their dimensions normal to the plane of the film. Thin films exhibit different physical properties than the same metal in bulk. One such property is that a thin film's crystal lattice orientation changes as it is annealed at temperatures ranging from room temperature to temperatures approaching their melting point. Knowledge on the physical properties of thin films can help to develop electronics with better structural integrity and more specific conductive properties. In order to conduct research on thin films, a sample is made inside a vacuum chamber in either high vacuum or ultra-high vacuum. The metal being studied is deposited using chemical vapor deposition (CVD) or using physical vapor deposition (PVD) via electron beam or magnetron sputtering.

1.2 History of Vacuum Systems

The goal of a vacuum system is to control sources of contamination within the experiment; more pure samples can be made when lower pressures are achieved. A combination of displacement, sorption and momentum transfer pumps is used in order to achieve vacuum. The 17th century saw the beginning of vacuum physics and technology. Galileo was among the first to conduct experiments to measure the forces required to produce vacuum with a piston in a cylinder. Torricelli succeeded in 1644 to produce vacuum experimentally by submerging the open end of a glass tube filled with mercury into a pool of mercury. The 1900's marked the development of vacuum systems for industry. The original oil-sealed rotary pump in Figure 1 was invented in 1905 by Walter Gaede and his design is still used for rotary pumps today [1]. This pump was a rotary mercury pump which could be motor driven. It could produce pressures in the 10^{-6} Torr range and was mass produced for uses in the lamp and vacuum-tube industries.

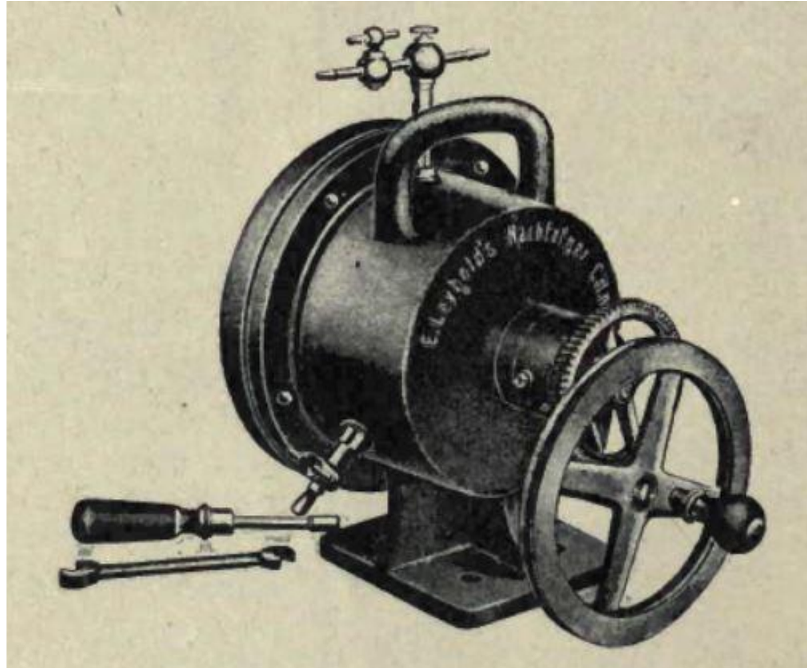

Figure 1. Gaede's Rotary Mercury Pump. Taken from [2].

The first molecular pump was proposed by Gaede in 1913 [3], but up until the late 1970's they were not used because of a lack of reliability and slow evacuation rate. Later, molecular pumps were modified and integrated into the design for a turbomolecular pump, the first of which was proposed by Becker in 1958 [4,5]. This design used rapidly rotating blades to evacuate the system, resulting in a much faster evacuation time compared to other pumps at the time. Now turbomolecular pumps spin up to 1500 Hz and can achieve pressures as low as 10^{-9} Torr.

The sputter-ion pump became available in 1958 and is used to achieve ultrahigh vacuum. The ion pump is a type of capture pump wherein the pumped gas molecules are trapped in the body of the pump. The gas molecules inside the chamber are ionized and then accelerated towards the wall of the pump. This is an especially popular design because it has no moving parts so no vibration is added to the system. Titanium is a common metal used in these pumps in order to capture gases in the chamber. The most common designs for this pump are based on a Penning cell [6].

With the many advancements in vacuum technologies, it is now possible to create a vacuum system in which experiments can be performed at low pressure. For thin films specifically, impurities can be reduced by depositing films in high or ultrahigh vacuum.

1.3 History of Thin Films and PVD

Due to interest in thin films and the potential for technological advances, research has been conducted on them since the mid 1800's [7-9]. In order to make and study thin films, significant advancements in Physical Vapor Deposition (PVD) systems have been made [10,11]. These advancements have allowed for much better control over the conditions in which films are made and the accuracy with which they are made. These improvements have increased the ability to further study the properties of thin films.

The concept of thin film deposition was believed to have been first found by accident by W. Grove in 1852 [7]. Grove was researching conducting properties of gases by looking at arching between electrodes in different atmospheres, while doing these experiments using the apparatus in Figure 2, a small amount of metal was deposited from the electrodes and formed a film that was noticed on the apparatus. This process of depositing films is now called sputtering. After this accident was noted, other scientists began to experiment with the concept. Such scientists include Faraday, Wright, and later, Edison. Faraday was interested in the optics of gold and other metallic thin films produced through electrical discharge [8]. Wright was one of the first scientists to begin work on producing thin films in vacuum and, like Faraday, he produced thin films of various metals through electric discharge [9]. Scientists such as Thomas Edison began to apply these deposition methods to commercial products. Specifically, Edison designed an apparatus seen in Figure 3, for the purpose of depositing thin films of metal onto phonograph-records and filed a number of patents pertaining to this invention [12-14]. This apparatus was used to deposit a thin layer of metal that was electrically conductive enough to perform electroplating. Edison wanted to electroplate phonograph records because he realized that it would make them stronger. He also applied for a more general apparatus that was for vacuously depositing metals [15].

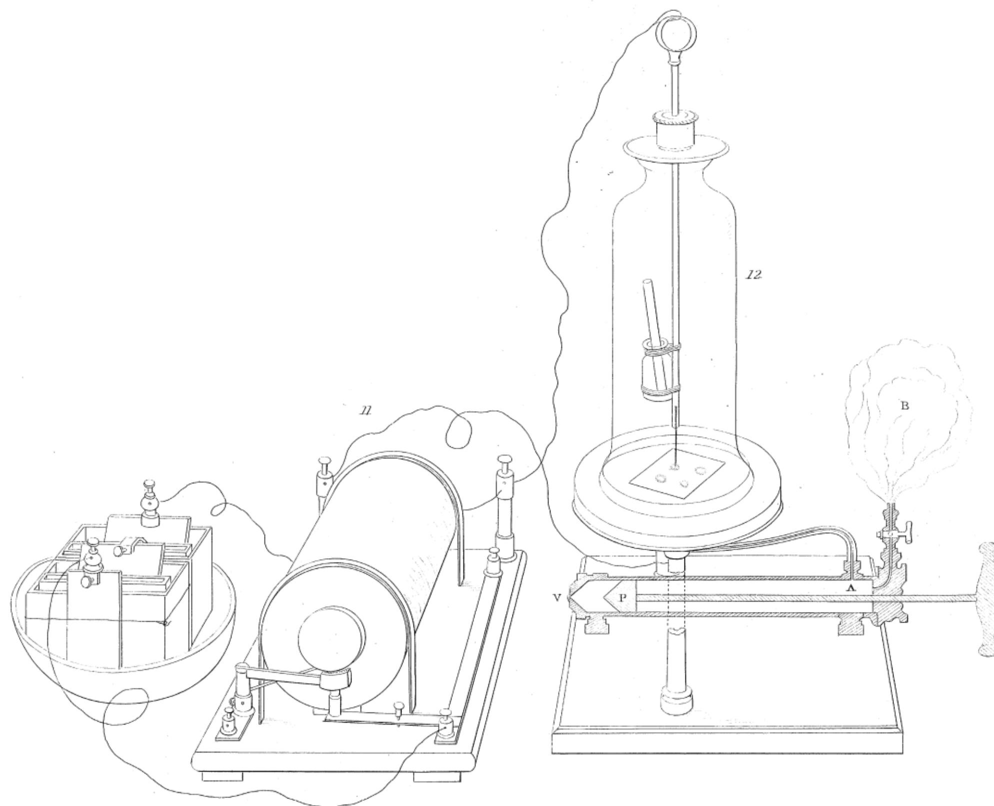

Figure 2. W. Grove's apparatus with which he discovered thin films. Grove used a tip of wire as the coating source and sputtered a deposit onto a polished silver surface held close to the wire. He noted a coating of silver on the surface of the wire the cathode of the circuit. Figure taken from [7].

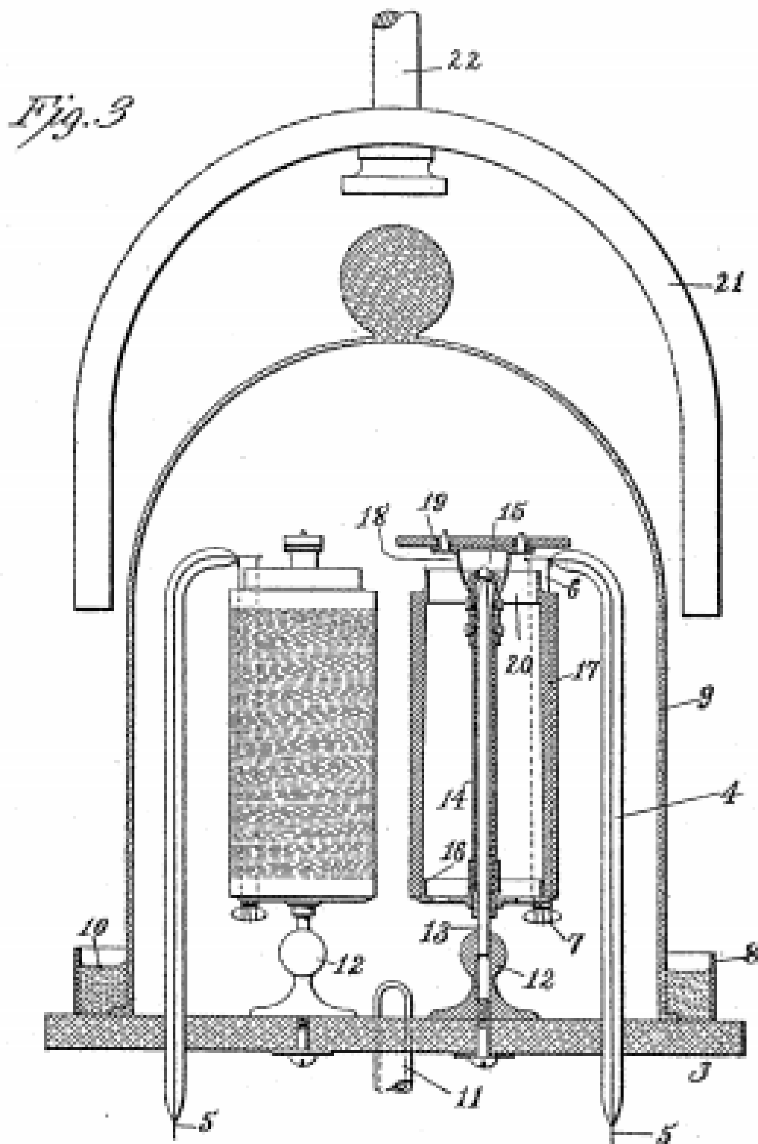

Figure 3. Edison's device for making phonographs. This device provides a base coating of metal for the production of phonograph records using PVD. The vacuum chamber was used to maintain as much purity as possible, and control the conditions in which the records were made more closely. Inside the chamber is the apparatus to be coated and electrodes with current running through them emitting atoms from their own mass. Figure taken from [15]

Physical vapor deposition works by evaporating the metal of interest, then condensing on a substrate. E-beam evaporation is one method of PVD by which the metal of interest is placed in a crucible inside a vacuum chamber at high or ultra-high vacuum. The sample is then heated through thermal emission of electrons from a filament to the appropriate temperature to vaporize. The filament can either be used to heat the crucible which in turn heats the metal as seen in Figure 4, or a magnetic field can be used to focus the electron beam directly at the sample as seen in Figure 5. This second method results in less heating of the system, but is a much more difficult process to use due to the need for highly accurate magnetic fields. The most common place for the substrate is directly above the crucible at the top of the chamber so that the metal evaporates and moves line-of-sight towards the substrate. When the metal turns to vapor, it travels straight out from the crucible then absorbs onto the substrate, forming a thin film. The film can be made with different thicknesses by controlling the evaporation rate of the metal and the time of exposure of the substrate.

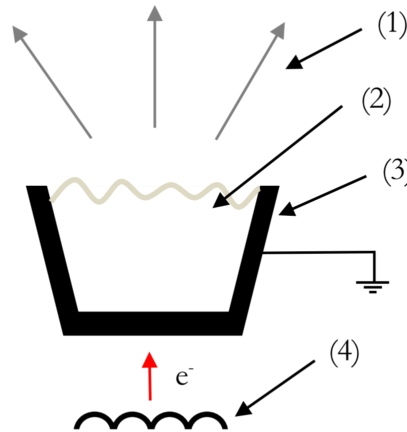

Figure 4. Electron beam vaporization via thermionic heating of a crucible. This configuration requires an electron source floating at high voltage (4) to be in close proximity to a conducting crucible (3) so that thermionic emission will occur and heat the evaporant (2) turning it to vapor (1).

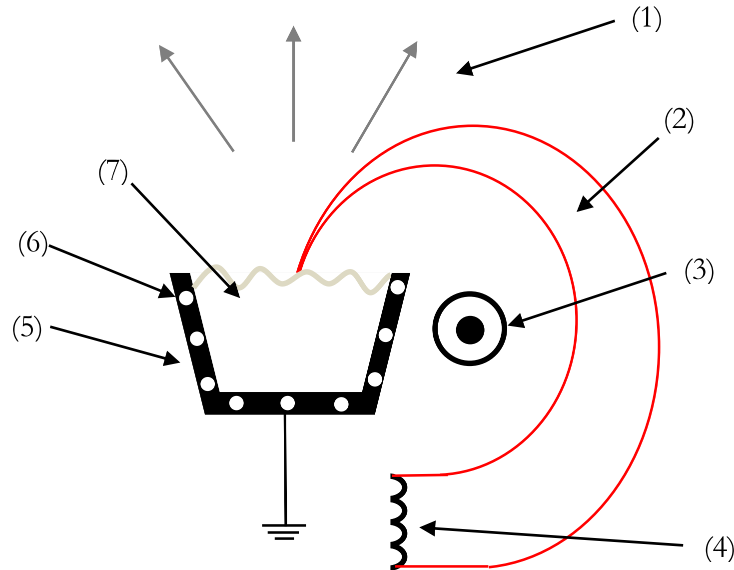

Figure 5. Focused E-Beam Evaporation configuration. The evaporant (1) is heated via thermionic heating from the electron beam (2) directly hitting the metal. The electron beam coming from the filament (4) is focused by a magnetic field (3) such that only the metal is being hit by the electron beam. The metal (7) sits in a crucible (5) that is water cooled (6) so that less contamination occurs during the heating process.

Another type of PVD is physical sputtering seen in Figure 6. This process is a non-thermal vaporization process in which the surface atoms of a metal are physically ejected from the bulk material solid surface by momentum transfer from an atomic-sized energetic bombarding particle, which is usually a gaseous ion accelerated from a plasma. This method is the most common way to deposit thin films for industrial purposes such as semiconductor material, magnetic films, and reflective coatings on compact disks [16].

1.4 Monitoring Evaporation Rate

In order to deposit films with the appropriate specifications for research, the rate of deposition needs to be monitored as the metal is being deposited. The quartz crystal microbalance (QCM) or crystal rate monitor is the most common evaporation rate monitor used in thin film deposition. The idea behind

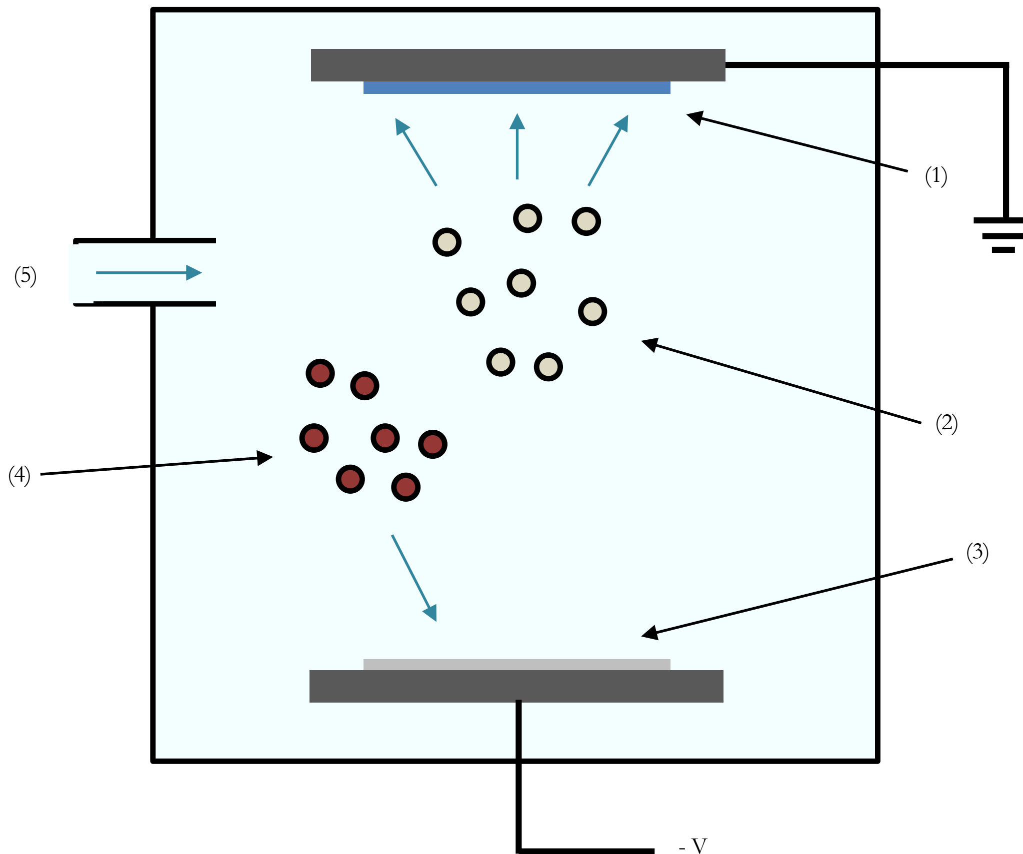

Figure 6. A physical sputtering system. A gaseous ion (4) is put into the chamber through the gas inlet (5). The ions are accelerated towards the target metal held at high negative voltage (3). Atoms are separted from the bulk and turn to vapor (2). The vapor then condenses on the grounded substrate (1).

these monitors is that they are made to oscillate at their resonance frequency. As metal is deposited onto the rate monitor, the mass of the quartz crystal changes, thus changing the frequency at which it oscillates. Based on the change in frequency, the rate of evaporation can be modelled. This monitor can be calibrated by comparing thickness measurements after deposition to the rate measured by the QCM. The problem with these types of monitors is that, after several depositions, metal accumulates on the quartz making it inaccurate and the quartz must be replaced. For this reason it is expensive and time consuming to maintain a working QCM.

1.5 Current Understanding of Thin Films

There has been particular interest in thin metal films that have a FCC lattice structure. This means that the atoms of the metal make a cube that has an atom at each vertex of the cube and on each face of it as seen in Figure 7. The lattice structure is created when these cubes of like orientation are repeated to form layers. In order to characterize the orientation of these cubic structures Miller indices are used. A Miller index is a three-value notation in which each number represents a value proportional to the inverse of a point on an orthogonal axis. Each point or intercept is defined as x_1, x_2, x_3 for the crystal structure's orthogonal axis 1, 2 and 3 seen in Figure 8. These points describe a plane that is parallel to the surface of the substrate and therefore describes the orientation of the orthogonal axis with respect to the substrate. As such, the Miller index $(h\ k\ l)$ is defined as $\left(\frac{1}{x_1}\ \frac{1}{x_2}\ \frac{1}{x_3}\right)$. Zero denotes that the plane does not intersect the particular axis at all. The plane described by the Miller index represents a surface parallel to the substrate, the orthogonal axis which this plane is described in is the axis for the crystal structure, so it tells us the orientation of the crystal with respect to the substrate's surface. The two main orientations observed in FCC thin metal films are (1 1 1) and (1 0 0) seen in Figure 9. The first, is when the cube made by the atoms is like a dice standing on its corner, the second is when the cube is sitting with its face flat on the normal plane. In thin films, arrays of cubes of like orientation tend to grow to form grains of like orientation creating a texture of a certain orientation.

It has been observed that thin metal films with FCC crystal lattice structure go through a transformation from a (1 1 1) to a (1 0 0) texture upon annealing [17-21]. When observing this transformation, it has been seen that deposited films which are sufficiently thin retain their (1 1 1) texture, while films that are sufficiently thick transform to have larger (1 0 0) textured grains [19]. These properties have been well established [19,21,22]. However, there is very little experimental evidence confirming any sort of model predicting these transformations.

The prevailing model of texture transformation of FCC cubic materials is given in [21] and basically says that the transformation is due to a minimization of energy between the strain and interface energies [22]. This model suggests that when a film is sufficiently thin, the (1 1 1) orientation will

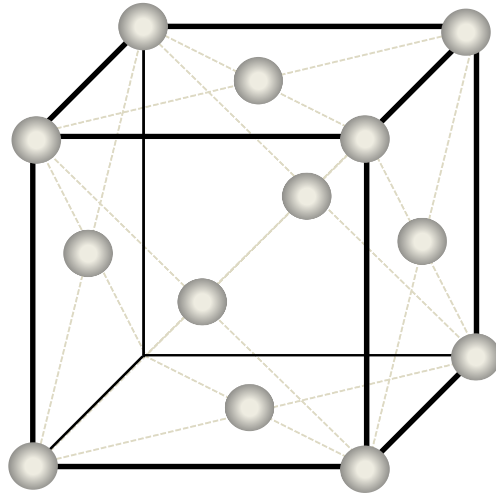

Figure 7. A faced-centered cubic crystal. The crystal is made up of a three dimensional array of these cubes that have atoms at each vertex and on each face of the cube.

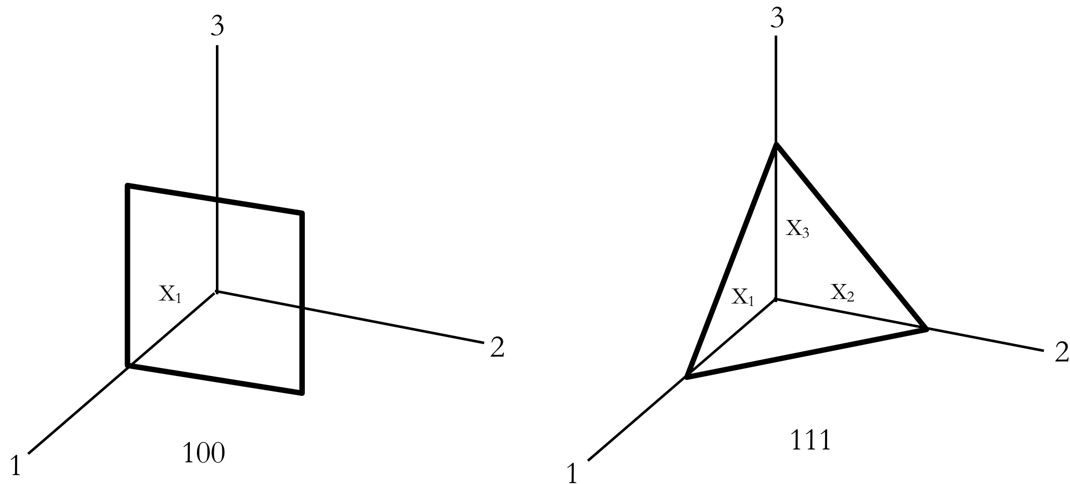

Figure 8. Diagram showing the planes that the (1 0 0) and (1 1 1) Miller indices describe. The (1 0 0) plane only intersects one axis, and the (1 1 1) plane intersects all three axes. The 1, 2 and 3 axes represent the coordinate system of the crystal structure and X_1, X_2, X_3 represent a plane parallel to the substrate.

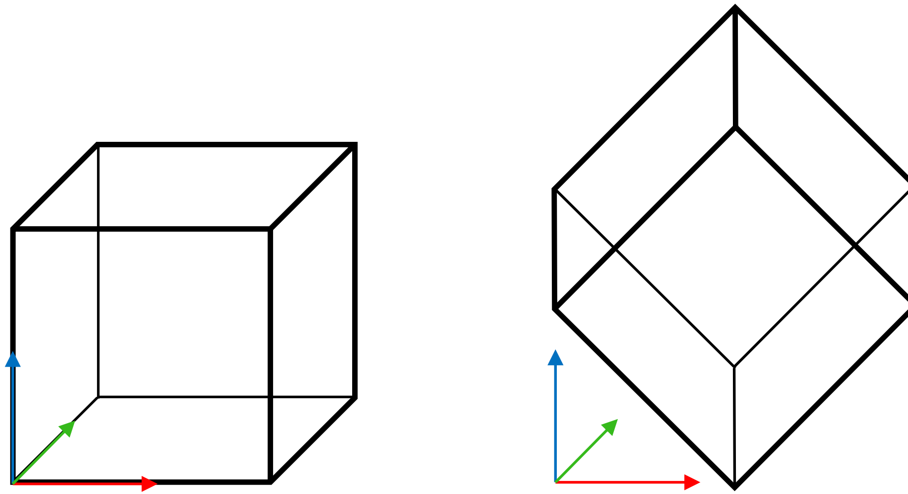

Figure 9. Miller indices, (1 0 0) and (1 1 1) orientations. These are the two main orientations found in FCC films. The (1 0 0) pictured left, is sitting with its face on the plane of the substrate. The (1 1 1) pictured right, is on its corner. The coordinate system shown is with respect to the substrate where the blue, z axis is normal to the substrate.

prevail because it has lower interface energy, but above some critical thickness (1 0 0) will prevail because it minimizes the strain energy. This transformation occurs because as the volume of the thin film increases, the interface energy per unit volume decreases while the strain energy per unit volume is constant with film thickness. This means that the critical thickness should occur when it is energetically favorable to minimize strain energy versus interface energy as seen in Figure 10.

There have been many studies showing that this model does not accurately describe why thin films go through this texture transformation [17, 21, 23]. All of these studies showed that although films would start with a high percentage of (1 1 1) orientation, there was still a mixture of many different orientations. The same was true after annealing. For thick films, the orientation ended at a high percentage of (1 0 0) orientation, but there were still other orientations in the film. The Baker group published extensive results that do not follow the predictions of the prevailing model for these

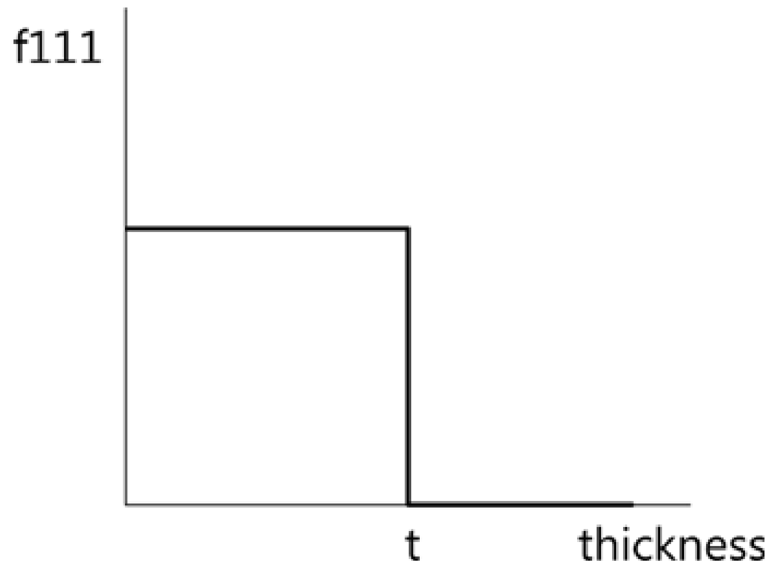

Figure 10. The current theory for texture transformation showing a critical thickness. This theory claims that for films that have been fully annealed, there is some critical thickness at which the films transform from being fully (1 1 1) orientation to fully (1 0 0). The y-axis shows the fractional volume of (1 1 1) to (1 0 0) orientation and the x-axis is the thickness of the sample. Taken from [24].

transformations, suggesting that the driving force of transformations can be attributed to a different kind of energy. In order to further study texture transformation, they looked at films of gradient thickness and recorded the transformation of films of varying thickness. They showed that although the transformation did depend on thickness, there was a range of thicknesses in which the transformation occurred, seen in Figure 11, instead of one critical thickness suggesting that the current theory does not adequately describe the transformation. This experiment allowed the group to compare the transformation results at different thicknesses because all of the samples were made in the same deposition run. They concluded that transformation rate depends strongly on the thickness of a film [21] but were unable to identify the driving force behind these transformations. This means that it is still unknown what actually causes these transformations to occur and more research needs to be done as to what is causing these transformations to occur.

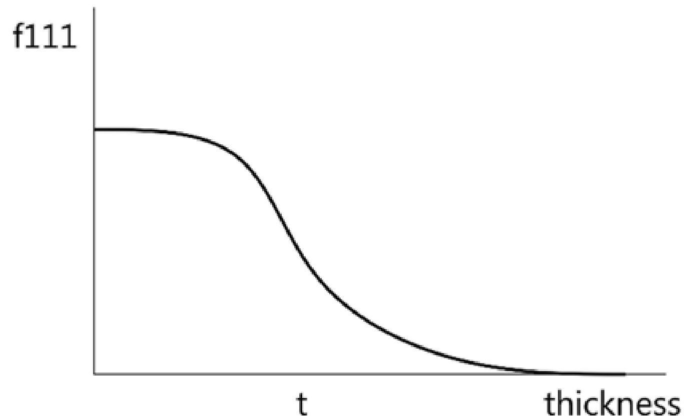

Figure 11. Data taken on texture transformation shows this trend. There is always a mixture of (1 1 1) and (1 0 0) crystals present but the ratio of the two changes with thickness. Taken from [24]

1.6 Thin Film Research at Houghton

It has been shown that comparing thin films that were produced during different deposition runs is very difficult to do. Unexplained differences have been found in such films that were produced in the same chamber under the same conditions [21]. As such, it is important to be able to study thin films that are produced during the same deposition run. To do so, Baker used a gradient thickness film in order to produce a film with multiple different thicknesses during one deposit. In order to study the effect thickness has on texture transformation, Houghton College is building a thin film deposition vacuum chamber pictured in Figure 12 that includes shutters that will allow gradated films to be produced. To produce these films, it was decided that the electron-beam method would be used. Houghton College is using a method similar to the one referred to as e-beam evaporation wherein electrons from a filament are focused onto the sample itself using a magnetic field, heating the sample through thermal emission of the electrons. The method of electron-beam evaporation being used follows the same principle, but rather than bending and focusing the electron beam with magnetic fields, a carbon crucible will be heated by the electron beam, which will then heat the metal. The reason for using this method is simply because the e-beam method is very costly to make, and maintenance is very difficult.

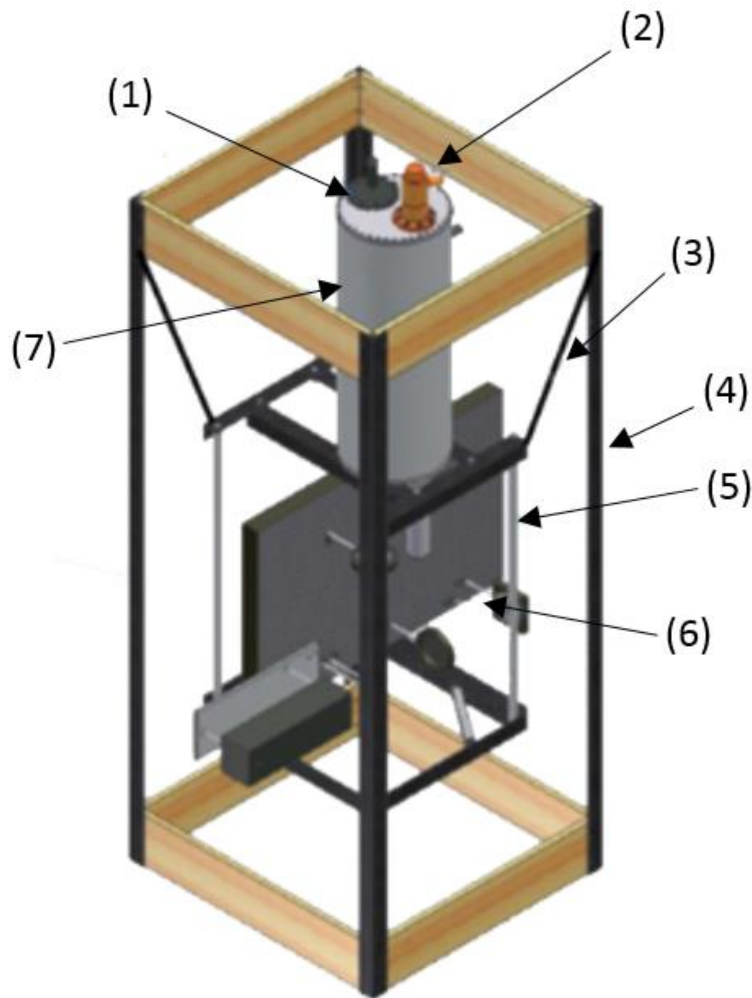

Figure 12. Houghton College PVD chamber showing locations of aspects of the chamber. (1) Rotary feedthrough and sample holder, (2) Turbomolecular pump, (3) isolating springs, (4) outer frame, (5) inner frame, (6) Houghton College interferometer, (7) deposition chamber. Figure taken from [25].

Houghton College hopes to continue the research of texture transformations in thin films with the completion of the deposition chamber. Other projects under construction that will allow for the study of the films produced are: an interferometer for measuring thickness and curvature of gradient films, an x-ray diffractometer for looking at the crystal structure and orientation of the films, and an atomic force microscope for studying roughness and grooving in thin films.

Chapter 2

APPARATUS

2.1 Introduction

Houghton College currently has a vacuum chamber that has produced thin silver films. The quality of these films has as of yet not been analyzed. The project includes the chamber itself with the necessary pumps to achieve high vacuum, the deposition block required to evaporate silver and other metals, the evaporation rate monitor to measure the rate at which a film is being deposited, and the ion mill for cleaning the substrate before deposition.

The chamber, seen in Figure 13, has multiple electrical feedthroughs, linear feedthroughs and rotary feedthroughs that can be used to manipulate shutters to make gradient films. There is also a window at the bottom of the chamber so that an interferometer can be placed underneath in order to measure in-situ topography of the thin films being deposited. In order to achieve vacuum, rubber gaskets are used on all feedthroughs. A three stage pumping process is used to achieve pressures on the order of 10^{-7} Torr.

2.2 Evaporator

2.2.1 Transformer and Rectifier Circuit

Houghton College uses a thermal vaporization method in order to deposit metals. The evaporant is placed in a carbon crucible held by a Macor block seen in Figure 14. The crucible is then heated via electron beam thermionic emission and the evaporant turns to vapor and absorbs onto the substrate. The electron source is a tungsten filament that has a current driven through it by a 12 V battery and floats at high voltage. The crucible is grounded which, with the large potential difference between crucible and filament, results in the thermionic emission. This emission current heats the carbon crucible by the kinetic energy of the electrons turning into thermal energy when they hit the crucible. Since the metal is placed inside the crucible, it also heats up. The emission current depends on both the potential difference between the crucible and filament and the current going through the filament.

As seen in Figure 15, the filament current is controlled by a variable power resistor connected to the 12 V battery so that different currents can easily be achieved.

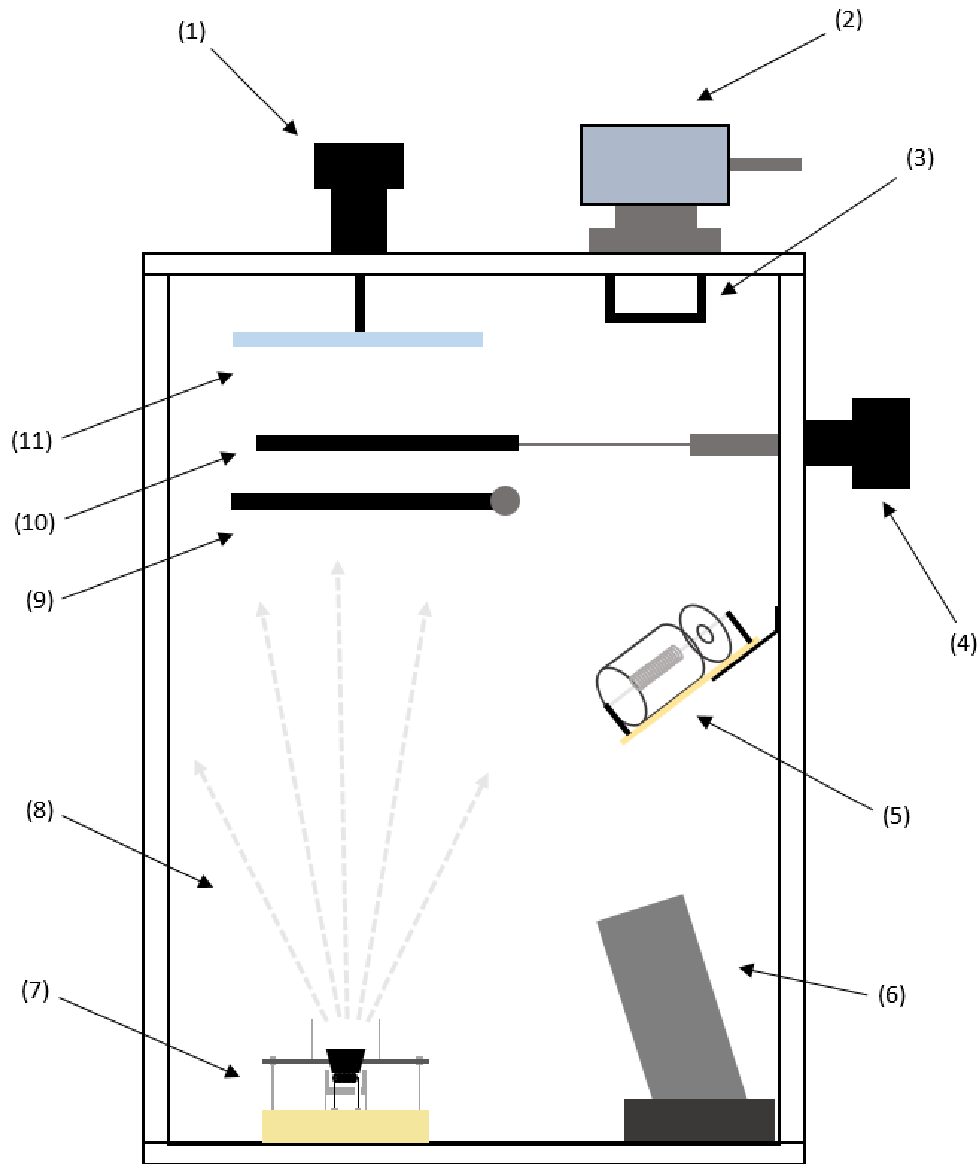

Figure 13. Inside of the deposition chamber. (1) rotary feedthrough that is attached to the sample holder, (2) turbomolecular pump, (3) turbo shield to prevent metal vapor from getting into the turbo, (4) linear feedthrough, (5) Evaporation Rate Monitor, (6) ion mill for cleaning the substrate, (7) evaporator, (8) silver vapor, (9) sample shutter, (10) linear shutter and (11) silicon substrate.

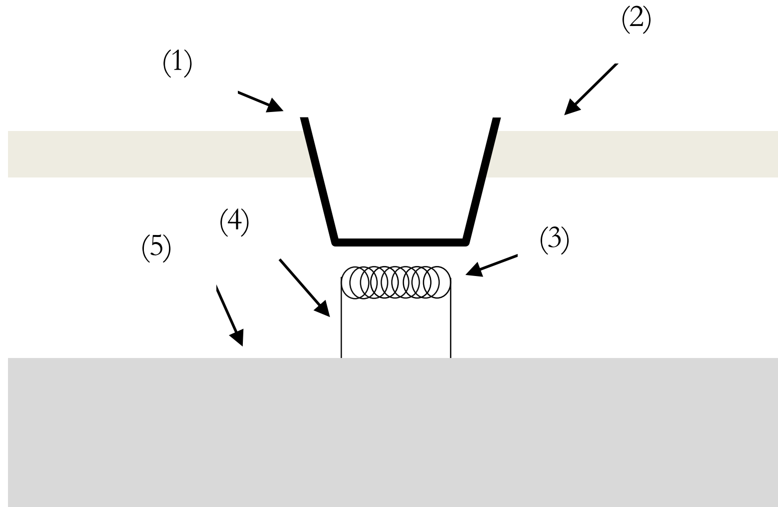

Figure 14. The evaporator. The carbon crucible (1) is grounded, the top Macor plate (2) holds the crucible, the filament (3) connected to stainless steel posts (4), emits electrons. Both the filament posts are screwed into the bottom Macor plate (5).

The first step in getting the deposition chamber functional was to create a circuit that could produce up to 5 kV DC and be able to supply sufficient emission current from the filament to the crucible. The current power supply is one which a variac connected to a transformer outputs high AC voltage and then a rectifier transforms the AC to DC voltage. The transformer was purchased so that a 120 V, 15 A variac could be attached to the transformer which could output one hundred times the variac voltage. Next, a full wave bridge rectifier circuit with 5 kV, 200 mA diodes and capacitors was used to convert the AC voltage. In order to be sure that the emission current supplied by the high voltage source will not blow out each component, diodes and capacitors are wired in parallel in order to reduce the current going through each. Upon testing, this circuit was successful at maintaining 5 kV and up to 180 mA. With a sufficient high voltage supply in place, a high voltage electrical feedthrough was added. This feedthrough is rated to 5 kV and 5A, allowing enough power to be supplied to the evaporator to deposit silver.

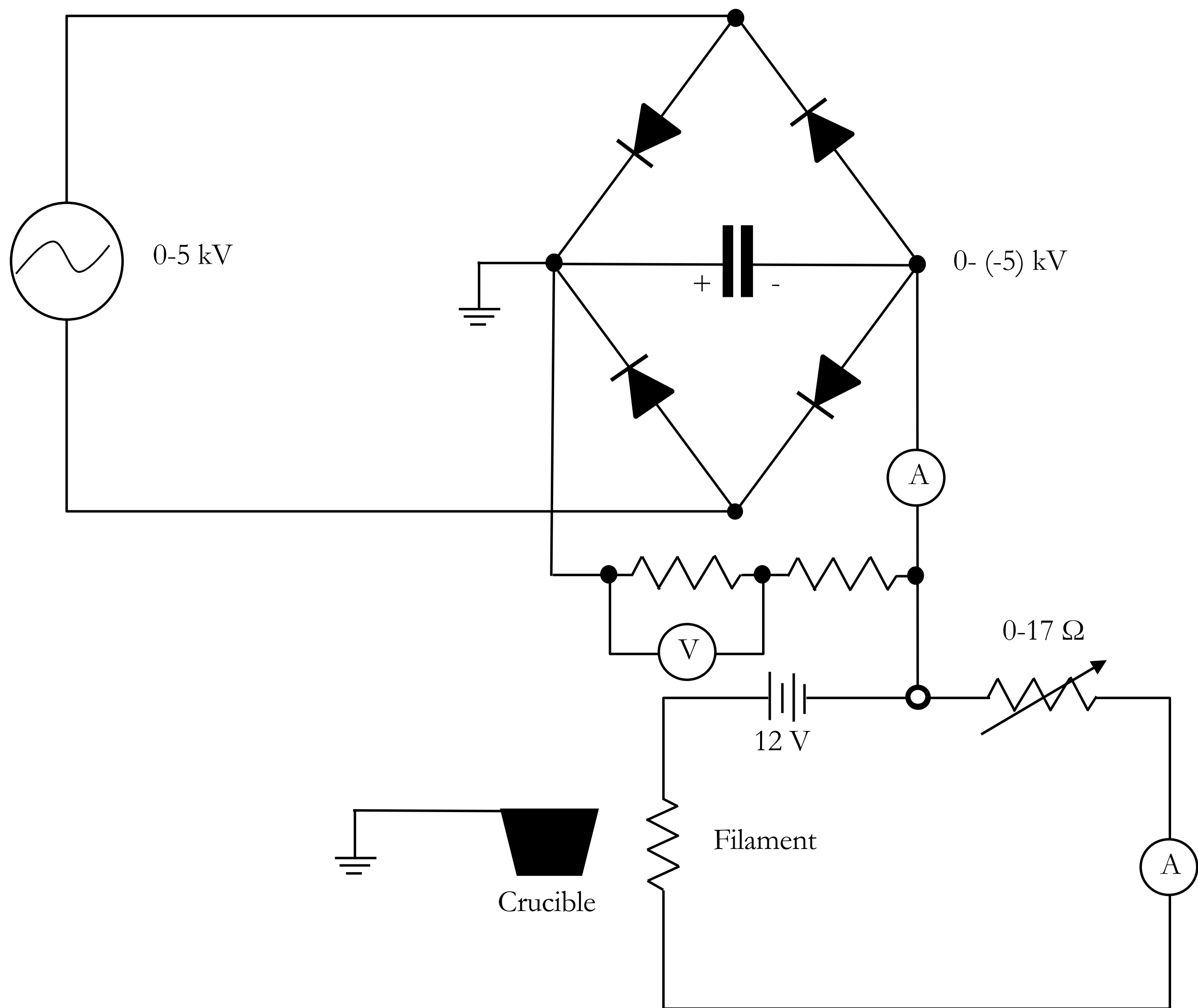

Figure 15. Circuit diagram for the entire electronics set-up for the evaporator. The rectifier is attached to the circuit driving the current of the filament, thus floating the filament at high voltage. A variable resistor attached to a 12 V battery is used to control the current across the filament.

2.2.2 Designing New Evaporator

For reasons that will be discussed in Chapter 3, it was decided that the evaporator needed to be modified as seen in . The first change was to make the top plate out of stainless steel instead of Macor. This plate includes a hole for the crucible made by drilling three separate holes so that there are only three small points of contact between the crucible and the steel. This new top plate, seen in Figure 17, is designed so that there is less thermal contact between the plate and crucible. This makes up for the fact that steel is more conductive than the Macor, so that the relative heating of each is the same. The second new feature on the evaporation block is a radiation shield made out of aluminum. This shield is made to sit on the bottom Macor block with the filament post feeding through two holes in the shield. One hole is insulated with ceramic piping, while the other is in contact with the post so that the entire shield will be at the same floating voltage as that side of the filament. A third feature is a chimney that sits on top of the steel plate such that the line of sight from crucible to windows and ion gauge is blocked. This was added so that silver would not condense on the window, blocking visibility, and so that silver would not get inside the ion gauge.

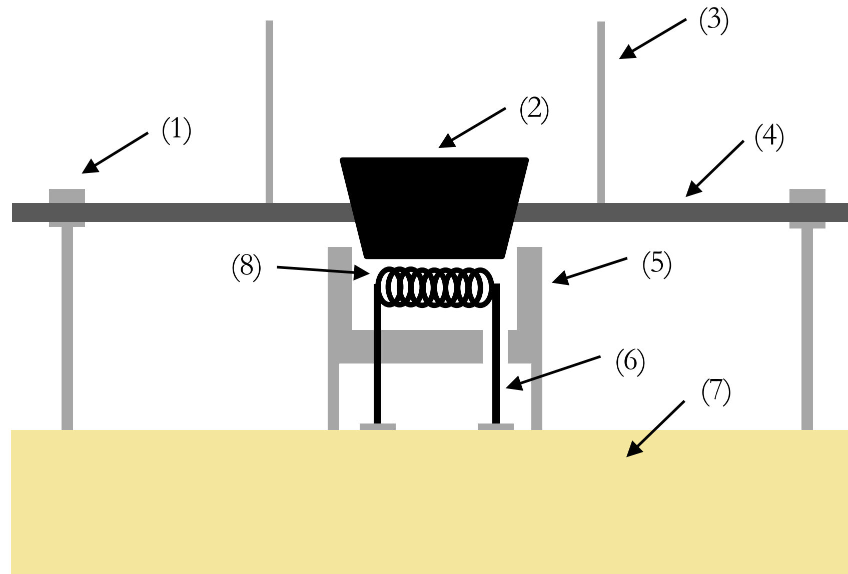

Figure 16. The new evaporator. (1) stainless steel bolts with nuts holding up the top plate, (2) the crucible, (3) molybdenum chimney, (4) stainless steel plate, (5) aluminum radiation shield, (6) stainless steel filament posts, (7) macor base, (8) tungsten filament.

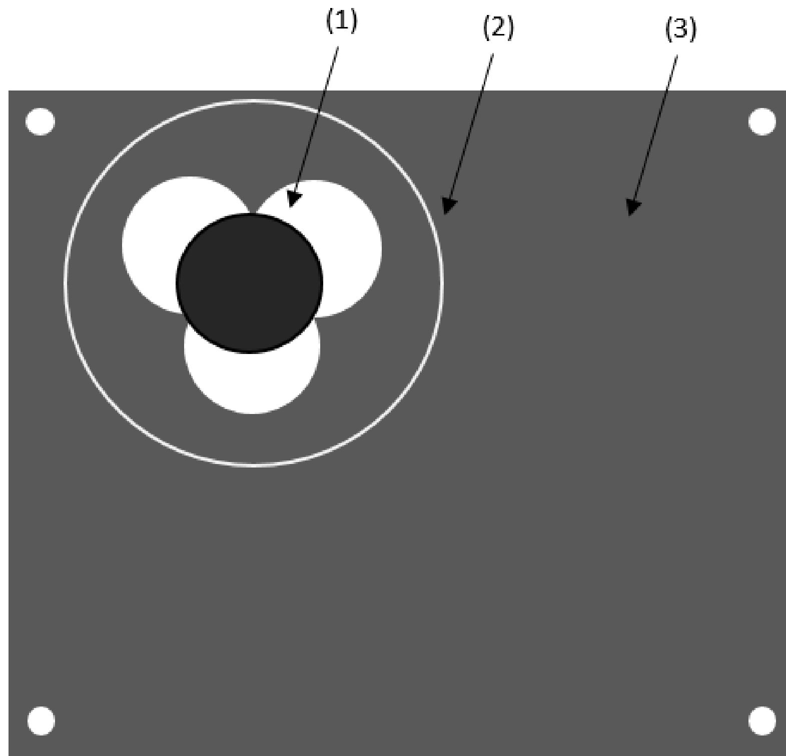

Figure 17. Top view of the top plate that holds the crucible. (1) crucible, (2) molybdenum chimney, (3) steel plate. This plate is designed to reduce the amount of contact between the crucible holder and the crucible itself in order to reduce heating the holder via thermal contact.

2.3 Rate Monitor

Houghton College has implemented a type of rate monitor that has not yet applied to a PVD system seen in and Figure 19. The Evaporation Rate Monitor (ERM), seen in Figure 20, described in a paper written by G.R. Giedd and M.H. Perkins published in 1960 [26] is the basis for Houghton College's rate monitor. This device is essentially a modified ion gauge, wherein a filament is surrounded by a cylinder held at a high positive voltage and the evaporated material is ionized by the filament and accelerated towards a collector held at negative voltage. The ionized material bombarding the collector causes a current to be induced in the collector. Since the current is directly proportional to the rate of ionized material, it can be measured in order to determine the evaporation rate of the metal itself.

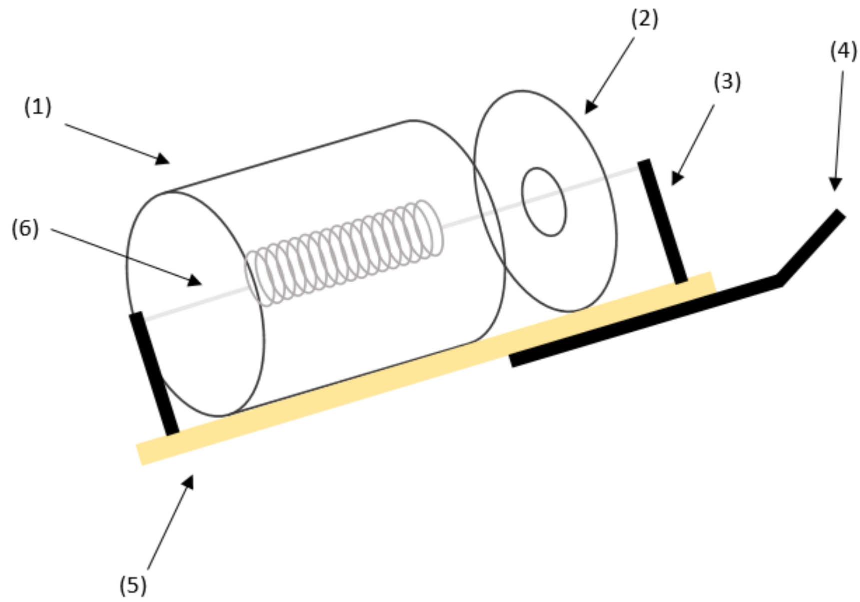

Figure 18. Diagram of Houghton College's Evaporation Rate Monitor (ERM). This is the design presented by Geidd and Perkins. (1) is the cylindrical anode made out of molybdenum, (2) the collector also made from molybdenum, (3) the stainless steel filament post, (4) steel mount, (5) Macor base, (6) tungsten filament.

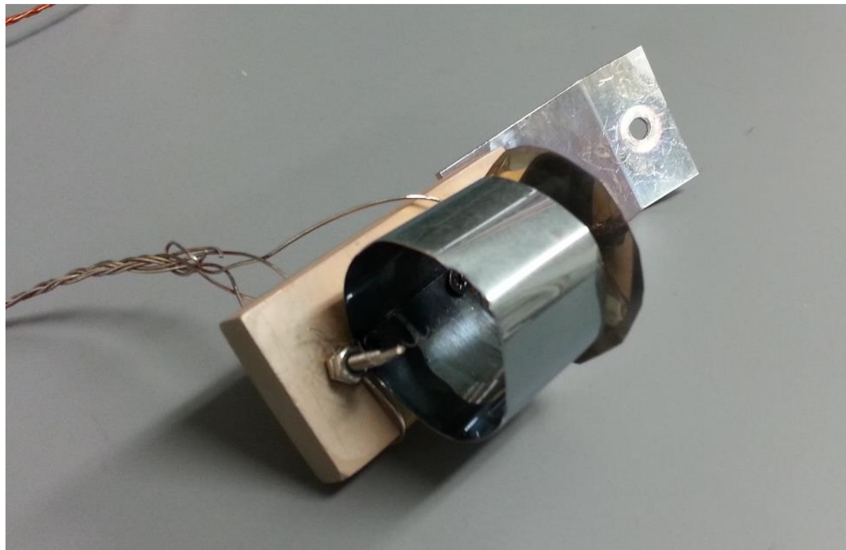

Figure 19. A Photo of Houghton College's Evaporation Rate Monitor (ERM). It is mounted half way up the chamber pointing towards the evaporator. This is the design presented by Geidd and Perkins.

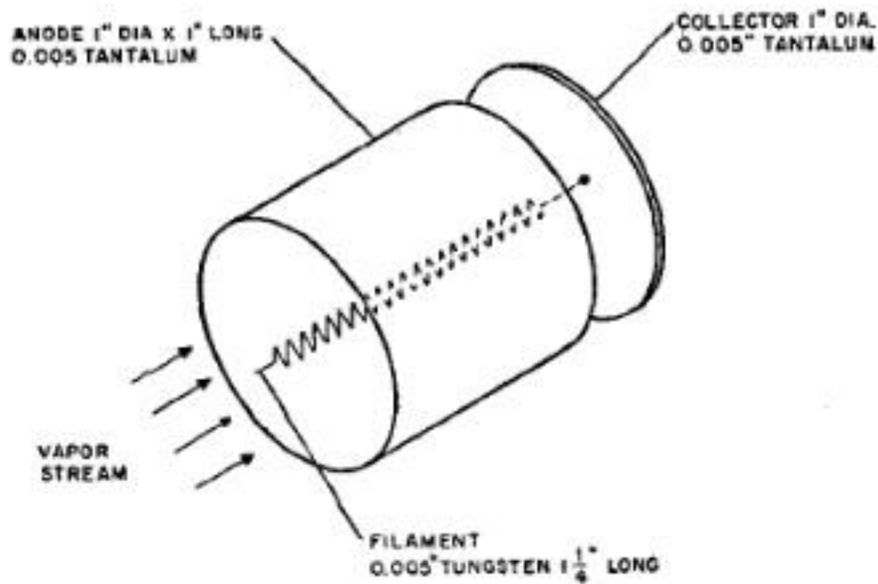

Figure 20. Diagram of Evaporation Rate Monitor (ERM) presented by Geidd and Perkins. Figure taken from reference [26].

2.4 Pumps

2.4.1 Rough

The first stage of the evacuation system is a rotary vane pump (RVP), depicted in Figure 21, which is connected to the chamber through the turbo pump and achieves a rough vacuum for the system. Once a pressure of approximately 10^{-3} Torr is achieved, the turbomolecular pump is turned on and the RVP becomes the backing pump for the turbo. The RVP works by the rotor and vane dividing the inner chamber of the pump into two variable volumes. As the rotor turns, gas flows into the enlarging chamber until it is sealed off by the second vane. The enclosed gas is then compressed until the output valve opens because the inside pressure overcomes atmospheric pressure. This process continues as gas gets sucked in the sorption and compressed gas exits the exhaust.

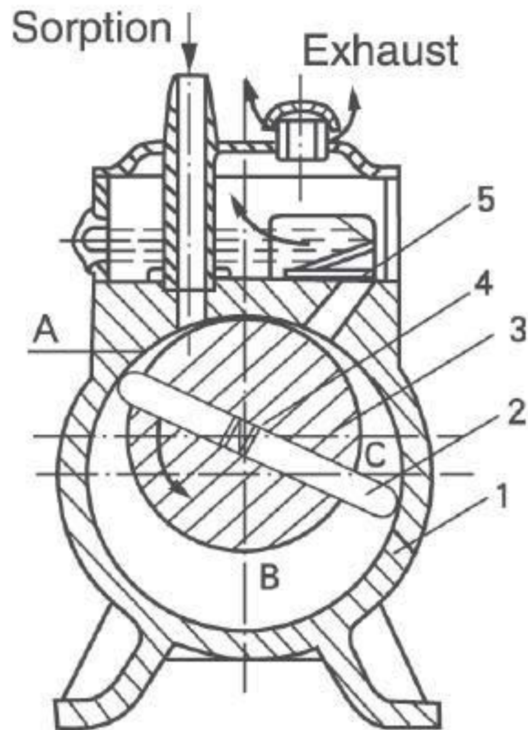

Figure 21. The Rotary Vane Pump. Components are the outer shell (1), the spring loaded vane (2), the inner rotor (3), the spring for the vane (4), and the output valve (5). Figure taken from [27].

2.4.2 Turbo

The turbomolecular pump shown in Figure 22 is the second stage to the vacuum system and is capable of bringing the system to high vacuum. This pump works by using alternating rotating and stationary blades causing gas molecules to flow at high velocities in one direction. The turbo cannot operate with too high pressure on the high pressure side, so the RVP is required to provide a backing pressure. With a lower pressure on the high pressure side of the turbo, the blades are allowed to spin more smoothly thus reducing the wear of the pump. Its operational range is from 10^{-3} to 10^{-9} Torr and it is responsible for bringing the chamber down to high vacuum. With the current chamber and pumping system, Houghton College has been able to achieve pressures as low as 5 x 10^{-8} Torr. While still using Viton rubber gaskets, this is approximately the lowest pressure that will be achieved.

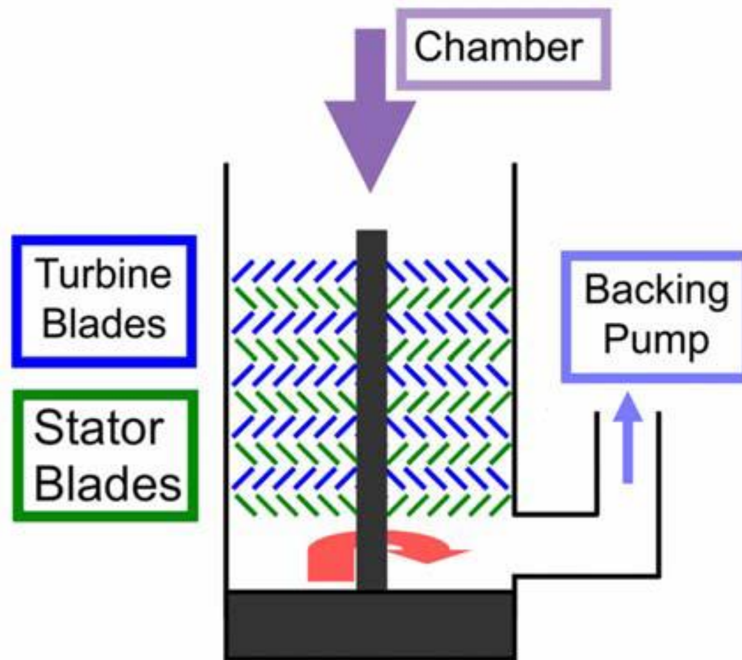

Figure 22. Cross-section diagram of the turbomolecular pump. This diagram shows the alternating rotor blades and stationary blades. These blades enable the pump to force gas through the pump without any flow of gas back into the chamber. Figure taken from [27].

Ion

Figure 23, in order to further lower the pressure of the system. The ion pump has been mounted but as it is not currently the focus of the project, it is not currently mounted. The ion pump has no moving parts and operates by applying a high potential difference across ambient molecules. The ionized molecules accelerate towards the wall and become trapped. A magnetic field is induced within the pump so that the ionized molecules spiral towards the wall so that they can ionize other particles as they travel towards the wall. This pump has the major benefit of having no moving parts. This benefit will be used when analyzing the topography of in-situ films. In order to reduce vibrations during analysis by the interferometer, the turbo pump will be turned off. However, since the ion gauge has no moving parts, it will be left on in order to maintain high vacuum.

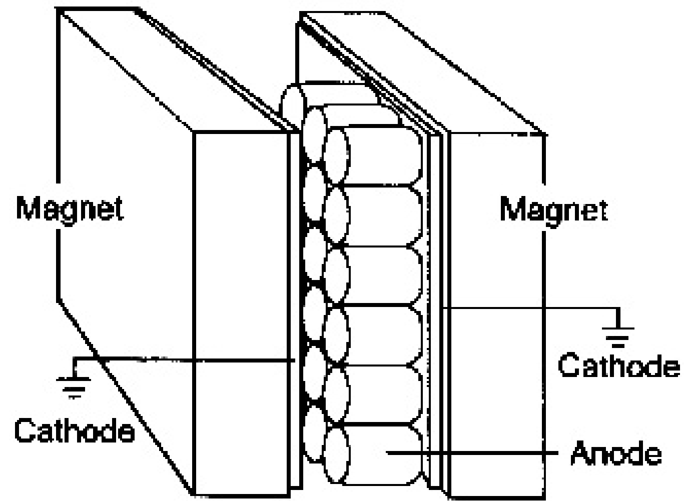

Figure 23. Diagram of an ion pump. Molecules go into the pump and are ionized. The ionized particles are then attracted to the grounded cathode and stick to it, eliminating them from the chamber's atmosphere. Taken from [28].

Chapter 3

ANALYSIS

3.1 Results

3.1.1 First Film

Houghton College deposited its first film on February 18, 2014. The purpose of making this film was to test the electronics to ensure that everything was working. The rate of deposition was not monitored and the thickness of the film was not measured. The success of this run was solely measured by the fact that silver was visibly deposited. Initially the electronics were set up as discussed in 2.2.1, but it was believed that the wire ribbon was shorting somewhere inside it. In order to test the electronics, the filament was grounded and the crucible was held at high negative voltage. The film was made by putting 1.9 A across the grounded filament, and floating the crucible at 3.5 kV, this resulted in an emission current of 60 mA. This voltage and current were the settings required to visibly see that the silver had melted, the only method used to tell if vaporization had occurred was by looking at the sample of silver. By going off of the current and voltage measured when the silver visibly melted, the power required to evaporate silver was 210 W. This deposition run allowed for the diagnosing of any flaws in the setup of the electronics and the deposition block itself, including the initial problem of the filament wires shorting to ground.

One issue that was found was that the high voltage feedthrough was arching across pins when voltage was higher than 3.5 kV, which was a surprise because the feedthrough is rated to 5 kV. Since a film was made at lower voltage than what made the feedthrough arch, it was decided that the feedthrough was acceptable and did not need to be changed. Another issue is that there was visible sparking inside the chamber near the filament, underneath the crucible. It was unknown why this was occurring, however it was decided that an effort needed to be made to clean the gap between the filament posts to ensure there was no residue causing any sort of connectivity. A final issue was that silver condensed on the windows of the chamber, therefore there was concern that silver could also affect the ion gauge monitoring the pressure of the chamber. It was decided that a chimney would be added to the

deposition block in order to ensure that line-of-sight from crucible to the low feedthroughs on the chamber was blocked. Some of this silver deposit could have also come from the electric field lines created when changing the ground from the crucible to the filament. This could result in an electric field changing the direction of the silver ions. Since the whole chamber was grounded, field lines could go in all directions causing the silver ions to also be sent in different directions.

3.1.2 Second Film

On September 19, 2014 a second film was deposited. This film was made at a base pressure of 4×10^{-7} Torr. The filament current was 2.18 A, and the voltage was set to -3.5 kV. This resulted in an emission current of 80 mA. Again, these measurements were noted when the silver had visibly melted, the power from the current and voltage was 280 W. This deposition run was hampered by both the high voltage and the filament current drifting, making it very difficult to control the power being supplied to the crucible. The pressure also steadily increased, and was finally the reason why the run was ended, when pressure reached 6×10^{-5} Torr. Upon venting it was found that indeed a film had been made, but the top ceramic block had cracked in multiple places, presumably due to too much heat. There was also a silver coating on the top block and around the block on the bottom of the chamber. This was probably because of shorting occurring causing electric field lines to direct the silver ions downwards.

After this deposition run, a new crucible holder needed to be built since the one used in this experiment was broken. The design of this was discussed in section 2.2.2. It was also decided that a more thorough degassing process would be used. This process would include baking the chamber to 235˚F and gradually turning the filament on while the chamber was hot. This process was included to avoid the pressure spikes experienced in this second deposition run.

3.1.3 Third Film

On December 12, 2014 a third film was deposited. This deposition run was meant to test the new triangular crucible holder. Some silver was deposited, but the film was opaque and had a yellowish hue to it. Both the current and voltage varied greatly through this run so a power was not calculated. It was

estimated that the power was in the same range as the first two runs with the voltage over -3kV and the emission current varying anywhere between 60 and 90 mA. There were multiple issues during this run, the biggest one being that the filament wire was arching to the triangular crucible holder which was at ground. It is believed that this resulted in loss of power heating the crucible and made it so a constant evaporation was not achieved. From this deposition run it was decided that the current evaporator design would be used. The steel top plate would provide sufficient distance from the filament leads as well as enough heat resistance. The radiation shield would also provide thermal radiation protection to the rest of the system as well as maintaining a higher crucible temperature.

3.1.4 Fourth Film

On March 20, 2015 a fourth film was deposited using the new evaporator design. The base pressure was 1.5×10^{-7} Torr, filament current was 2.2 A, high voltage was -1.5 kV, and emission current was 115 mA. The power from this run at 172.5 W showed that the power required to melt the silver had decreased, meaning that the two modifications to reduce heat loss worked. This result was still measured by seeing that the silver had melted so there is some significant error when trying to compare the power run to run. During deposition there was still a significant pressure spike and was again the reason for ending the run. It has also been noticed that the pressure does not go back down very quickly after a pressure spike, so some buffer time is needed before turning the evaporator back on.

Chapter 4

CONCLUSION

4.1 Current Status

The deposition chamber has been tested and shown to be able to produce thin films that are intended to be of a single thickness, although thickness and topography have not been measured. The evacuation process is now consistent and achieves pressures of approximately 5 x 10^{-8} Torr using a roughing pump and a turbomolecular pump. The baking process has been refined which allows for lower pressures to be achieved and therefore a cleaner environment for deposition. The electronics are also now working properly such that a constant voltage and emission current are achieved. This means that in the future it will be possible to perform more precisely controlled runs which will allow for gradient films of specific thicknesses to be made. The ERM has been mounted inside the chamber, and it has been wired properly, however no emission current has been achieved between the filament and anode.

4.2 Future Plans

The next steps for the Deposition Chamber will include the implementation of the Evaporation Rate Monitor and calibrating the system to perform more precise deposition runs. Monitoring the rate of evaporation will be important in confirming that a constant rate of deposition is achieved. Maintaining constant but different rates will be important for performing experiments that look at texture transformation.

In order to do this, further tests will have to be performed while measuring the current off of the ERM. If a constant current can be achieved then it will be known that a constant evaporation rate has been achieved. The ERM will also have to be calibrated by measuring the thickness of the silver deposited. Houghton does not yet have to capabilities to measure thickness. However, it is hoped that

the interferometer will soon be capable of topographical images of stepped films. This will allow determination of thickness and calibration of ERM.

Appendix A

PROCEDURES

A.1 Evacuation Procedure

- Ensure rough valve is closed by tightening the nozzle
- Ensure turbo vent is closed by tightening the nozzle on the side of the turbo
- Ensure turbo valve is open, line up "open" line on handle at the bottom of the turbo such that it is vertical.
- Turn pressure controller on, switch to pressure gauge display.
- Turn rough pump on by turning on power strip
- Open rough valve by loosening nozzle all the way
- Wait for rough pressure to reach somewhere between 10^{-2} Torr and 10^{-3} Torr
- Turn water cooling for turbo on
- Turn pumping unit for turbo on
- Turn ion gauge and controller on
- Once pressure is between 10^{-6} Torr and 10^{-7} Torr, turn bake on (See Bake Procedure)

A.2 Venting Procedure

- Ensure all electronics are off
- Close rough valve
- Turn rough pump off
- Turn turbo pump off
- If turbo hits resonance frequency and starts vibrating, allow some air in to raise the pressure
- Once pressure is between 10^{-6} Torr and 10^{-7} Torr, turn bake on (See Bake Procedure)

A.3 Bake Procedure

- Plug in temperature controller, set to 300˚F
- Plug variac into 120 V AC

- Plug resistor strips are covered by aluminum foil
- Ensure resistor strips are covered by aluminum foil
- Turn variac up in steps to allow for gradual heating
- Once pressure is between 10^{-6} Torr and 10^{-7} Torr, turn bake on (See Bake Procedure)
    - Start variac at 20 V
    - Once temperature is between 100˚F and 110˚F, turn variac up to 40 V
    - Once temperature is between 150˚F and 160˚F, turn variac up to 60 V. Exceding 60 V will result in the variac current maxing out and blowing a fuse.
- Throughout this process make sure the pressure does not rise above 5×10^{-5} Torr
- Once pressure has stabilized, degas the evaporator filament with bake on
- Gradually turn filament current up, ensuring pressure does not spike
- Once filament current is at 2 A with stabilized pressure, turn bake off
- Allow the chamber to cool with the evaporator filament on so that it stays clean

A.4 Deposition Procedure

- Check initial pressure
- Make sure chamber is grounded
- Turn on all multimeters, need to monitor:
    - Filament current
    - High voltage
    - Variac current
    - Current from HV supply
    - Current from crucible to ground
- Turn evaporator filament current up to 2.2 A
- Turn HV supply on (turn on variac switch)
- Begin turning up variac voltage, monitoring pressure
- Turn voltage up until the desired evaporation rate is achieved

References

[1] W. Gaede U. K. Patent No. 17,741 (7 September, 1905).

[2] S. Dushman, *Production and Measurement of High Vacuum*. (The General Electric Review, Schenectady (1922).

[3] W. Gaede Ann. Phys. (Leipzig), **43 (4)**, 337 (1913).

[4] W. Becker, Vak. Tech. **16**, 625 (1958).

[5] W. Becker, *Turbo-Molecular Pump*, US Patent 3,477,381 (1969).

[6] F.M Penning, Philips Technical Review, **2**, 201 (1937).

[7] W.R. Grove, Philosophical Transactions of the Royal Society, **142**, 87 (1852).

[8] M. Faraday, Phil. Trans., **147**, 145 (1857).

[9] A. W. Wright, Amer. J. Sci. and Arts, **13**, 49 (1877).

[10] Milton Ohring, *Materials Science of Thin Films* (Academic Press, San Diego, 2002).

[11] L.B. Freund and S. Suresh, *Thin Film Materials Stress, Defect Formation, and Surface Evolution.* (University Press, Cambridge, 2009).

[12] T. A. Edison, U. S. Patent No. 484,582 (18 October 1892).

[13] T. A. Edison, U. S. Patent No. 488,189 (20 December 1892).

[14] T. A. Edison, U. S. Patent No. 680,520 (13 August, 1901).

[15] T. A. Edison, U. S. Patent No. 767,216 (9 August, 1904).

[16] D. M. Mattox, *Handbook of Physical Vapor Deposition (PVD) Processing* (Noyes Publications, Park Ridge, New Jersey, 1998), p. 6.

[17] J. Greiser, D. Muller, P. Mullner, C. V. Thompson, E. Arzt, Scripta Mat., **41**, 709 (1999).

[18] K. Vanstreels, S. H. Brongersma, Z. Tokei, L. Carbonell, W. De Ceuninck, J. D'Haen, M. D'Olieslaeger, J. Mater. Res., **23**, 643 (2008).

[19] P. Sonnweber-Ribic, P. Gruber, G. Dehm, E. Arzt, Acta Materialia, **55**, 765 (2007).

[20] C. Polop, C. Rosiepen, S. Bleikamp, R. Drese, J. Mayer, A. Dimyati, T. Michely. New J. Phys., **9**, 74 (2007).

[21] S. P. Baker, B. Hoffman, L. Timian, A. Silvernail, E. Ellis, Acta Materialia, **61**, 7121 (2013).

[22] C.V. Thompson, R. Carel. Material Science and Engineering, **B32**, 211 (1995).

[23] J. Greiser, P. Muyllner, E. Arzt. Acta Materialia, **49**, 1041 (2001).

[24] J. Mertzlufft, Undergraduate Thesis (Houghton College, New York, 2013, unpublished).

[25] K. Aikens, Undergraduate Thesis (Houghton College, New York, 2009, unpublished).

[26] G.R. Geidd and M.H. Perkins, The Review of Scientific Instruments, **31** (7), 773 (1960).

[27] http://www.sfpumps.com.cn/en_ProductShow.asp?ProductID=43.

[28] http://www.cae2k.com/howto.html.